═══REVIEW COMMONS MANUSCRIPT═══

IMPORTANT:

- Manuscripts submitted to Review Commons are peer reviewed in a journal-agnostic way.
- Upon transfer of the peer reviewed preprint to a journal, the referee reports will be available in full to the handling editor.
- The identity of the referees will NOT be communicated to the authors unless the reviewers choose to sign their report.
- The identity of the referee will be confidentially disclosed to any affiliate journals to which the manuscript is transferred.

GUIDELINES:

- For reviewers: https://www.reviewcommons.org/reviewers
- For authors: https://www.reviewcommons.org/authors

CONTACT:

The Review Commons office can be contacted directly at: office@reviewcommons.org

Neuroepithelial depletion schedules cessation of neurogenesis in the *Drosophila* optic lobes

Phuong-Khanh Nguyen[1,3], Louise Y Cheng[1,2,3,#]

1. Peter MacCallum Cancer Centre, Melbourne, VIC 3000, Australia
2. Sir Peter MacCallum Department of Oncology, The University of Melbourne, VIC 3010, Australia
3. Department of Anatomy and Physiology, The University of Melbourne, VIC 3010, Australia

Corresponding author

Email: louise.cheng@petermac.org

Keywords: *Drosophila*, medulla neuroblast, gliogenesis, neuroepithelium

Running title: medulla neuroblast termination

Abstract

The brain is consisted of diverse neurons arising from a limited number of neural stem cells. *Drosophila* neural stem cells called neuroblasts (NBs) produces specific neural lineages of various lineage sizes depending on their location in the brain. In the *Drosophila* visual processing centre - the optic lobes (OLs), medulla NBs derived from the neuroepithelium (NE) give rise to neurons and glia cells of the medulla cortex. The timing and the mechanisms responsible for the cessation of medulla NBs are so far not known. In this study, we show that the termination of medulla NBs during pupal development is determined by the exhaustion of the NE stem cell pool. Altering NE-NB transition during larval neurogenesis disrupts the timely termination of medulla NBs. Medulla NBs terminate neurogenesis via a combination of cell death, terminal symmetric division, and a switch to gliogenesis. We show that temporal progression is not required for the termination of medulla NBs. The timing of NB cessation can be altered through the acquisition of a glial cell fate via Glial cells missing, or through conversion to type II NB cell fate via Tailless, or by inhibition of differentiation via Prospero knockdown. As the *Drosophila* OL shares a similar mode of division with mammalian neurogenesis, determining how and when these progenitors cease proliferation during development can have important implications for mammalian brain size determination and regulation of its overall function.

Introduction

The central nervous system (CNS) is the cognitive control centre of the body and is generated by neural stem cells (NSCs) during development. *Drosophila* NSCs, called neuroblasts (NBs), produce different neural and glial types and subtypes that contribute to the formation of the adult brain. The cellular diversity of the CNS is determined in a region-specific manner, via differential control of NB division mode and temporal identity (reviewed by Harding & White, 2018). The majority of NBs are Type I NBs located in the ventral nerve cord (VNC) and the central brain (CB). They divide asymmetrically to generate a NB and a smaller ganglion mother cell (GMC), that undergoes terminal differentiation to give rise to neurons or glial cells (Harding & White, 2018). In addition, there are eight Type II NBs located on the dorsal surface of the CB, where NBs asymmetrically divide to give rise to a NB and an intermediate neural progenitor (INP) (Bello et al., 2008; Boone & Doe, 2008; Bowman et al., 2008). INPs undergo maturation prior to additional rounds of asymmetric division, to give rise to neurons and glial cells.

The optic lobes (OLs) of the brain are the visual processing centre of the adult fly brain (Figure 1A). During neural development, neurogenesis in the OLs takes place in two proliferation centres: the inner and the outer proliferation centres, which produce different neural cell types that populate the various cortexes of the visual system (Sato *et al*, 2019; Apitz & Salecker, 2014). In the outer proliferation centre (OPC), medulla NBs are generated from a pseudostratified neuroepithelium through a differentiating "proneural wave" (Figure 1A') (Egger et al., 2007; Li et al., 2013; Yasugi et al., 2008). This proneural wave is characterised by the expression of proneural factors such as Lethal of scute (L'sc) which precedes NB generation from NE cells (Yasugi et al., 2008). During early larval stages, OPC NE cells undergo symmetric cell divisions to expand the progenitor population. By early-third instar, progression of the proneural wave is initiated in the NE cells at the medial edge, leading to their differentiation into medulla NBs. Medulla NBs sequentially express a series of temporal transcription factors (Konstantinides et al., 2022; Li et al., 2013; Zhu et al., 2022). During the early-mid temporal stages, NBs divide asymmetrically to produce two neurons, upon acquiring the terminal temporal identity, NBs switch to become glioblasts that produce glial cells (Zhu *et al*, 2022).

At the end of neurogenesis, NBs of different neural lineages are eliminated through distinct mechanisms. For instance, type I NBs in the VNC and the CB exit the cell cycle and

terminally differentiate at around 24 hr after pupal formation (APF), whereas type I abdominal NBs are eliminated via apoptosis prior to pupation (Maurange *et al*, 2008; Bello *et al*, 2003; Ito & Hotta, 1992). Mushroom body NBs are the last NBs to undergo termination, and they do so through apoptosis or autophagy prior to adult eclosion (Siegrist *et al*, 2010; Pahl *et al*, 2019). So far, the timing and mode by which medulla NBs terminate is not known; furthermore, it is unclear whether the temporal series, which schedules NB cessation in other NB lineages (Maurange et al., 2008; Syed et al., 2017) is also involved in the termination of medulla NBs.

Here, we find that medulla NBs terminate between 12-18 hr APF. Unlike other NB lineages, the timing of medulla NB cessation is mainly regulated by the depletion of the NE pool. The exhaustion of the NE during pupal development results in the lack of the formation of new NBs. Hence, altered NE-NB transition is sufficient to change the timing of NB termination. Additionally, we demonstrate that medulla NBs terminate via a combination of cell death, size-symmetric terminal differentiation and a switch to gliogenesis. While medulla NBs undergo temporal transitions, the temporal series is not required for NB termination. However, overexpression of Tll, Gcm and knockdown of Pros prevents timely NB cessation during the pupal stages.

87 **Results**

88 **Medulla NBs terminate during early pupal development.**

89 To characterize the timing at which medulla NBs are eliminated during pupal development,
90 we first assessed the number of NBs in the OPC using the pan-NB marker Deadpan (Dpn).
91 We found that the number of NBs was significantly reduced between 12-18 hr APF and by 30
92 hr APF, all the NBs were eliminated (Figure 1B-C).

93 In most regions of the CNS, NB termination is associated with a reduction in cell
94 growth and proliferation rate, scheduled by a peak of ecdysone between larval and pupal
95 development (Homem *et al*, 2014). To test if ecdysone signalling plays a role in the
96 termination of medulla NBs, we first looked at the expression of the ecdysone receptor (EcR)
97 in the medulla NBs at 12 hr APF, prior to the reduction in the number of medulla NBs in the
98 OL. Immunostainings showed that EcR is expressed at very low levels in the medulla NBs at
99 12 hr APF (Supplementary Figure 1A). Additionally, when EcR was knocked down via
100 RNAi in the medulla NBs with *eyR16F10-GAL4,* which is expressed in a subset of medulla
101 NBs and their progeny (Veen *et al*, 2023), we could not detect any persistent NBs at 24 hr
102 APF (Supplementary Figure 1B, C, E). A similar phenotype was observed using a dominant
103 negative form of EcR (EcR^{DN}) (Supplementary Figure 1D, E). Together, these data suggest
104 that ecdysone signalling in the medulla NBs is not required for their cessation during pupal
105 development.

106 During larval development, NBs regrow to their original size after each division
107 empowered by aerobic glycolysis providing the NBs with energy and metabolites for rapid cell
108 growth and proliferation (Homem *et al*, 2014; Maurange *et al*, 2008). To assess if a reduction
109 in cell size also precedes NB elimination in the medulla, we monitored the nuclear size of NBs
110 marked by Dpn. Between 12-18 hr APF when the majority of medulla NBs disappear, we found
111 that there was a significant reduction in the nuclear sizes of the medulla NBs (Figure 1D-E),
112 suggesting that decreased cell growth precedes the cessation of medulla NB. However,
113 increasing cellular growth through the overexpression of a constitutive active form of the PI3K
114 catalytic subunit Dp110 ($dp110^{CAAX}$) (Leevers et al., 1996), or the activation of the cellular
115 growth regulator Myc (Rust *et al*, 2018) did not prolong NB persistence in the OL at 24 hr APF
116 (Supplementary Figure 1F, G, J, data not shown).

117 In type I NBs of the CB and VNC, it was previously shown that NB termination is
118 dependent on core components of the mediator complex, which promote key enzymes to
119 increase oxidative phosphorylation (OxPhos) to slow down NB regrowth (Homem *et al*, 2014).
120 Nevertheless, neither inhibition of OxPhos itself via the knockdown of Complex I (Ameele &

121 Brand, 2019), nor the knockdown of Med27 via RNAi (Homem *et al*, 2014), a component of
122 the Mediator complex, significantly affected medulla NB persistence at 24 hr APF
123 (Supplementary Figure 1H-J). As such, although cell size reduction coincides with NB
124 elimination during pupal development, a decrease in cell growth, OxPhos, and the ecdysone-
125 induced Mediator complex are not required for the termination of medulla NBs.
126
127 **The depletion of the NE determines the timing of medulla NB cessation.**
128 NBs of the medulla are continuously generated from NE cells from mid-late larval
129 development by the proneural wave (Egger et al., 2007; Yasugi et al., 2008). To assess if NE
130 depletion during pupal stages is linked to the cessation of medulla NBs, we first characterised
131 the volume of NE cells during pupal development. From 12 hr to 24 hr APF, the NE
132 gradually decreased in volume, concordant with the reduction in the number of medulla NBs
133 during this time window (Figure 2A-B, Figure 1B-C). This suggests that the depletion of the
134 progenitor NE pool may drive the cessation of medulla NBs.
135 To test if the depletion of the NE can change the timing of NB termination, we
136 manipulated Notch signalling, a negative regulator of the NE-NB transition (Egger et al.,
137 2010; Wang et al., 2011; Yasugi et al., 2010), where Notch signalling promotes NE self-
138 renewal and prevents their differentiation into NBs (Egger et al., 2010; Wang et al., 2011;
139 Yasugi et al., 2010). Control and *notch* RNAi clones were induced in the medulla NE at 24 hr
140 after larval hatching (ALH) and examined at 96 hr ALH. Control clones spanned the NE and
141 NB regions, demarcated by a sharp NE-NB boundary indicated by PatJ (NE) and Mira (NB)
142 (Figure 2D). In contrast, *notch* RNAi clones consisted mostly of only NBs, suggesting that
143 Notch inhibition has caused an accelerated NE-NB transition (Figure 2E) (Egger et al., 2010;
144 Wang et al., 2011; Yasugi et al., 2010). By 12 hr APF, we found that *notch* RNAi clones
145 were smaller in size and contained very few NBs compared to control (Figure 2F-H). Thus, it
146 is likely that an accelerated NE-NB transition caused by *notch* RNAi resulted in a premature
147 depletion of the NE which in turn led to the early termination of NBs. To test this further, we
148 overexpressed the proneural gene *lethal of scute* (*l'sc*), which has also been shown to
149 promote NE-NB transition during the larval stages (Yasugi et al., 2008) (Figure 2I). Similar
150 to *notch* RNAi clones, *l'sc* overexpression caused medulla NBs to undergo premature
151 termination at 12 hr APF (Figure 2J-K). Together, our data indicate that the premature
152 depletion of the NE results in earlier medulla NB termination.
153 Conversely, we found that the overexpression clones of Notch signalling via N^{ACT}
154 caused a delay in the NE-NB transition, resulting in clones consisting only of NE cells (and

155 no NBs) at 96 hr ALH (Figure 2L). We only started to observe NBs in N^{ACT} clones in the OLs
156 (Figure 2M, n = 8/8 lobes) at 72 hr APF, a time point where control medulla NBs have long
157 disappeared. These medulla NBs continued to persist into the adult OL (data not shown).
158 Together, our results suggest that early depletion of the NE results in the early cessation of
159 medulla NBs, whereas delayed formation of the NB from the NE results in late termination of
160 medulla NBs. Thus, the timing of the NE-NB transition determines when medulla NBs
161 terminate.
162
163 **Medulla NBs cease divisions via cell death.**
164 Next, we examined how medulla NBs undergo termination. First, we examined mechanisms
165 that are responsible for the termination of other NB lineages. Mushroom Body NBs are the
166 last NBs to undergo termination (Ito & Hotta, 1992). These NBs are eliminated via a
167 combination of apoptosis and autophagy (Siegrist *et al*, 2010). To test if medulla NBs
168 terminate via similar mechanisms, we first assessed cell death, where we assayed for the
169 expression of the apoptotic marker Caspase-1 (Dcp-1) in the medulla NBs marked by
170 Dpn::GFP. At 12 hr APF, we observed that some NBs expressed Dcp-1 (Figure 3A). To test
171 if apoptosis is required for the termination of medulla NBs, we inhibited cell death via the
172 overexpression of the baculovirus anti-apoptotic gene *p35* in clones as well as in medulla
173 NBs using *eyR16F10-GAL4*. Upon the inhibition of cell death, we observed a small number
174 of persistent NBs at 24 hr APF through both approaches (Figure 3B-D, Supplementary Figure
175 2A-B, E). However, no persistent NBs were found at 48 hr APF, suggesting that additional
176 factors may be involved to terminate medulla NBs (Supplementary Figure 2D, n = 5/5 lobes).
177 Next, we asked if autophagy is required to eliminate medulla NBs. To address this,
178 we inhibited autophagy via the expression of a RNAi against Atg1 in the medulla NBs with
179 *eyR16F10-GAL4* (Xu *et al*, 2015). We found that the timing of medulla NB termination was
180 not significantly affected by the inhibition of autophagy (Supplementary Figure 2C, E).
181 Together, our data suggest that cell death, and not autophagy, makes a minor contribution to
182 medulla NB termination.
183
184 **Medulla NBs undergo Pros-mediated termination.**
185 In type I NBs of the VNC, the nuclear localisation of a differentiation factor called Prospero
186 (Pros) precedes NB termination via size-symmetric cell division (Choksi et al., 2006; Li et
187 al., 2013; Maurange et al., 2008). To assess if medulla NBs also undergo Pros-mediated
188 terminal differentiation, we first examined Pros expression together with the pan-NB reporter

189 Dpn::GFP at 12 hr APF. We found that many Dpn$^+$ NBs expressed nuclear Pros (Figure 4A).
190 Then, we examined the expressions of Dpn::GFP with Miranda (Mira) marks mature NBs
191 and asymmetric cell division at 12 hr APF. Interestingly, we occasionally observed some
192 small Dpn$^+$ Mira$^-$ cells, that form doublets (Figure 4B), which we think are likely to be
193 progenies of NB symmetric divisions. Therefore, it is possible that medulla NBs also undergo
194 size symmetric divisions via Pros localisation like NBs of other lineages. To test if Pros is
195 required for the termination of medulla NBs, we induced *pros* RNAi clones (Shaw *et al*,
196 2018). This manipulation caused the formation of ectopic NBs in the deep layers of the
197 medulla where neurons reside during late larval stages (Figure 4C-B). In the *pros RNAi*
198 clones, many persistent NBs were found at 24 hr APF in contrast to the control (Figure 4E-
199 G). Together, our data suggest Pros is required to promote differentiation of the medulla NBs,
200 and consequently shut down medulla neurogenesis during pupal life (Figure 4H).
201
202 **Tailless is involved in controlling the timing of medulla NB termination.**
203 In the OL, medulla NBs sequentially express an array of temporal transcription factors as
204 they age to promote cellular diversity (Konstantinides et al., 2022; Li et al., 2013; Zhu et al.,
205 2022). The simplified temporal series includes Homothorax (Hth), Eyeless (Ey), Sloppy-
206 paired (Slp), Dichaete (D) and Tailless (Tll) (Figure 5A). It was previously shown that
207 nuclear Pros localisation occurred during the Tll$^+$ temporal window (Li et al., 2013); and that
208 the glial regulatory gene, Gcm, is expressed in the Tll$^+$ NBs prior a switch from neurogenesis
209 to gliogenesis (Konstantinides et al., 2022; Li et al., 2013; Zhu et al., 2022).
210 At 12 hr APF, we found some Tll$^+$ NBs were also *gcm*$^+$ (*gcm*-lacZ, Vincent *et al*,
211 1996) (Figure 5B), indicating that a neurogenic to gliogenic switch could also contribute
212 towards the disappearance of NBs at this time point. Consistent with this, at 12 hr APF, we
213 observed some superficially located Dpn$^+$ NBs that expressed both the differentiation marker
214 Pros and *gcm*-lacZ (Figure 5C, yellow arrowheads), suggesting that these NBs could be
215 undergoing a NB to glioblast cell fate transition. Deeper within the medulla, we found *gcm*$^+$
216 cells which express neither Dpn nor Pros (Figure 5C, white arrowhead), that are likely to be
217 the progenies of the glioblasts. Finally, we found a few medially located Dpn$^+$ NBs that
218 expressed Pros but not *gcm*-lacZ (Figure 5G, red arrowhead). This is consistent with what we
219 observed in Figure 4A-B, where some NBs undergo terminal differentiation through likely
220 via symmetric cell division.
221 To test if members of the temporal transcription factor series can alter NB persistence
222 and prevent the neurogenic to gliogenic switch, we first examined the role of Tll, which

223 defines the temporal window where terminal differentiation as well as the gliogenic switch
224 occur (Li et al., 2013; Zhu et al., 2022). First, we induced *tll* overexpression clones and found
225 that *tll* overexpression caused the formation of ectopic NBs in the larval CNS (Figure 5D, and
226 these NBs persisted at 24h APF (Figure 5E, n = 4/4 lobes). *tll* overexpression has been
227 previously shown to convert type I NBs to a type II NB cell fate that are capable of tumour
228 formation in type I NBs of the CB (Hakes & Brand, 2020). Indeed, we found that the *tll*
229 overexpressing NBs were mostly $Dpn^{+}Ase^{-}$ which is characteristic of type II NBs (Figure 5D-
230 E). Therefore, it is possible that *tll* overexpression caused type I to type II conversions that
231 accounts for why these clones failed to undergo termination on time.
232 Consistent with reports that Tll is not required for glial production in the larval
233 medulla NBs (Zhu et al., 2022), we found that inhibition of *tll* via a validated RNAi (Hakes &
234 Brand, 2020) was not able to alter the number of glial cells in the larval medulla
235 (Supplementary Figure 3A, B, E), nor the timing of medulla NB termination in pupal stages
236 (Supplementary Figure 3C, D, F). Moreover, the knockdown of *tll* did not alter the number of
237 NBs undergoing cell death assayed via Dcp-1 expression (Supplementary figure 3G-H) nor
238 the expression of Pros which promotes terminal size symmetric divisions (Supplementary
239 figure 3I-J). Together, while Tll is not required for medulla NB termination, ectopic
240 expression of Tll can induce persistent NBs. Furthermore, Tll acts independently of cell death
241 and symmetric NB termination mechanisms.
242 To assess whether early temporal transcription factors are required for the termination
243 of medulla NBs, we overexpressed Hth and inhibited Ey or Scarecrow (Scro) (Konstantinides
244 et al., 2022; Zhu et al., 2022) via RNAi in clones, which prevents the progression through the
245 temporal series. Nevertheless, none of these manipulations influenced the timing of NB
246 termination (data not shown). Taken together, altering temporal progression is not sufficient
247 to affect the timing of medulla NB termination in the pupal stages.
248
249 **Gcm-induced gliogenic switch can affect the timing of NB termination.**
250 We next assessed if manipulating the gliogenic switch can affect the timing of medulla NB
251 termination. Here, we induced *gcm* overexpression clones using a reagent previously
252 validated in Zhu et al., 2022. This manipulation was able to induce the formation of ectopic
253 glial cells during larval neurogenesis (Figure 5F-G). At 12 hr APF, we recovered
254 significantly fewer NBs in the OL upon *gcm* overexpression (Figure 5H-J), suggesting that
255 the induction of a gliogenic switch can cause precocious medulla NB termination. To assess if
256 the downregulation of *gcm* can cause prolonged NB persistence in the medulla, we knocked

257 down *gcm* using a previously validated RNAi (Zhu *et al*, 2022) in clones. This manipulation
258 was able to inhibit the expression of the glial cell marker Repo in clones during larval stages
259 (Supplementary figure 3K-L). However, no persistent medulla NBs was found at 24 hr APF
260 (Supplementary figure 3M-N, n = 5/5 lobes). This suggests that while the downregulation of
261 *gcm* is not sufficient to induce NB persistence, *gcm* overexpression can cause a neurogenic to
262 gliogenic switch and thereby, premature termination of NBs.
263

264 **Discussion**

265 Robust brain development requires the tight coordination between stem cell maintenance and
266 differentiation. In the *Drosophila* OL, there are two main stem cell pools, the NE cells that
267 divide symmetrically, and the NBs. Medulla NBs are derived from the OPC NE via the
268 proneural wave, which switch to asymmetric division where they self-renew and give rise to
269 GMCs that will produce post-mitotic neurons and glial cells of the medulla cortex (Egger et
270 al., 2007; Li et al., 2013; Yasugi et al., 2008). Our study shows that during early pupal
271 development, medulla NBs terminate via a combination of mechanisms including cell death,
272 Pros-mediated differentiation and a switch from neurogenesis to gliogenesis. While factors
273 such as ecdysone signalling and OxPhos of the NBs are involved in NB termination in other
274 lineages outside of the OL (Homem et al., 2014; Syed et al., 2017; van den Ameele & Brand,
275 2019; Yang et al., 2017), we found that these factors do not play a significant role in the
276 termination of medulla NBs. Instead, the main regulator of the timely NB cessation in the
277 pupal medulla is regulated by the timing of the conversion of NE-NB conversion during
278 larval stages. Intriguingly, while a specific cascade of temporal identity transcription factors
279 in the medulla NBs has been shown to generate the cellular diversity of medulla neurons and
280 glia (Konstantinides et al., 2022; Li et al., 2013; Zhu et al., 2022), temporal progression in the
281 medulla NBs appears dispensable for the timing of NB cessation in the pupal stages (Figure
282 6). Diseases such as microcephaly are mediated by the premature depletion of the NE pool, or
283 through a precocious commitment to neurogenic divisions (Götz & Huttner, 2005).
284 Consistent with this, our data present evidence that during development, the regulation of the
285 NE stem cell pool, and its timely conversion into NSCs is of critical importance to the overall
286 size and function of the brain.

287 **NE-NB transition determines the timely termination of medulla NBs.**

288 Our data support a model whereby once the NE pool is exhausted, no new NBs can be
289 generated. NBs transit through their temporal series to terminally differentiate to become

290 glial cells or neurons, which marks the end of medulla neurogenesis. Thus, unlike type I NB
291 lineages in which NB termination is scheduled by ecdysone signalling-mediated temporal
292 progression at the level of the NBs (Syed et al., 2017; Yang et al., 2017), in the OL, NB
293 termination is pre-determined in the NE. In the OL, besides medulla NBs, NE cells also
294 sequentially express an array of temporal factors, such as Chinmo and Broad downstream of
295 ecdysone signalling (Arain et al., 2022; Dillard et al., 2018; Lanet et al., 2013; Zhou et al.,
296 2019). Moreover, inhibiting the temporal Chinmo-to-Broad expression switch in the NE was
297 shown to delay the NE-NB transition, resulting in tumours with persistent NBs in the adult
298 OLs (Dillard et al., 2018; Zhou et al., 2019). The differences in the regulation of NB
299 termination in the OL medulla versus other lineages may be due to some fundamental
300 differences in the origins of these NBs. For example, in the OL, NBs are derived from the
301 NE, that undergoes rapid growth during larval development (Egger et al., 2007; Lanet et al.,
302 2013; Yasugi et al., 2008). Therefore, NB termination in the OL is scheduled at the level of
303 the NE, likely by the activation of ecdysone signalling during late larval development. In
304 contrast, NBs from other lineages are produced directly from the neuroectoderm in the
305 embryo without undergoing the transition from the NE (Harding & White, 2018). Hence,
306 their termination mechanism acts predominantly in the NBs during pupal development.
307 **Cell death makes a small contribution to NB termination.**
308 Consistent with previous reports, we found that cell death occurred in a subset of medulla
309 NBs at 12 hr APF (Hara *et al*, 2018). However, inhibition of cell death did not fully prevent
310 medulla NBs from termination in the pharate OLs (Supplementary Figure 2D), suggesting
311 that NBs can adopt alternative routes for timely termination before adulthood. From our data,
312 it is not yet clear whether a specific subset of medulla NBs undergo cell death. Although the
313 timing of cell death in the medulla NBs coincides with a small pulse of ecdysone around 10
314 hr APF (Riddiford, 1993), we showed that inhibition of ecdysone signalling in the medulla
315 NBs did not phenocopy the inhibition of apoptosis (Supplementary Figure 1B-E). Therefore,
316 unlike neurons in the OL which require ecdysone signalling for cell death during pupal
317 development (Hara et al., 2013), medulla NBs undergo cell death independently of ecdysone
318 signalling. Altogether, while some NBs terminate proliferation through cell death, it is likely
319 that cell death of the NBs makes a minor contribution to the termination of neurogenesis in
320 the medulla.
321 **A neurogenic-gliogenic switch and symmetric divisions cause NB cessation.**
322 Our data show that many medulla NBs displayed nuclear Pros expression during early pupal
323 stages (Figure 3A). Consistent with the essential role of Pros in promoting differentiation

324 (Choksi et al., 2006; Maurange et al., 2008), *pros* knockdown caused the persistence of the
325 NBs in the pupal OLs (Figure 3C-G), similar to other regions of the brain. In addition to
326 differentiation, another mechanism responsible for the cessation of neurogenesis, is the
327 commencement of gliogenesis. We found glioblasts in the early pupal medulla, which make
328 glial cells at the end of the temporal transcription factor series, express the NB marker Dpn,
329 the glial marker Gcm as well as the differentiation marker Pros (Figure 5B-C). As such, it is
330 possible that similar to the embryonic glioblasts, Pros is required for glial cell fate acquisition
331 via Gcm (Freeman & Doe, 2001; Ragone et al., 2001). As Gcm knockdown did not induce
332 any persistent medulla NBs during pupal stages (Supplementary Figure 3M-N), the presence
333 of Pros may likely induce symmetric division of the NBs, resulting in their termination.
334 Together, cell death, symmetric cell division and a gliogenic switch appear to be employed as
335 fail-safe mechanisms that help to eliminate the NB progenitor pool in the pupal OL. Hence, it
336 would be interesting to explore in the future the cross-regulatory relationship between these
337 termination programs.
338
339

340 **Materials and Methods**

341

342 **Fly husbandry**

343 Fly stocks were reared on standard media at 25°C. For larval dissection, brains were
344 dissected at wandering L3 stages (120 hr ALH). For pupal dissection, white pupae were
345 selected and allow to age until the desired stages (12 hr, 24 hr, 30 hr, 48 hr, and 72 hr
346 APF).

347 Wildtype fly was *w*^{1118}. *eyR16F10-GAL4* (BL 48737) was used to induce expression of
348 transgenes in a subset of medulla NBs and their progeny from larval development (Veen
349 *et al*, 2023). Knockdown and overexpression clones were induced by flip-out system using
350 *hsFLP,act>CD2>GAL4;UAS-Dcr2,UAS-GFP* (a gift from Lei Zhang). Flip-out clones were
351 induced at 24 hr ALH for 10 min. *FRT42D;UAS-tll* clones were induced using the
352 MARCM system: *UAS-mCD8::GFP,hsFLP;FRT42D, tub-GAL80; tub-GAL4* (a gift from
353 Alex Gould). Clones were induced at 48 hr ALH for 15 min.

354 The fly strains used were as followed: *Dpn::GFP* (Morin *et al*, 2001), *FRT42D* (a
355 gift from Alex Gould), *gcm-lacZ* (BL 5445), *Tll::EGFP* (BL 30874), *Pros::GFP* (VDRC
356 318463), *UAS-Atg1 RNAi* (BL 26731), *UAS-dp110*^{CAAX} (BL 25908), *UAS-EcR RNAi*
357 (VDRC 37058), *UAS-EcR*^{DN} (BL 9451), *UAS-gcm* (BL 5446), *UAS-gcm RNAi* (VDRC
358 110539), *UAS-l'sc* (BL 51670), *UAS-lacZ* (BL 8529), *UAS-mCherry RNAi* (BL 35785),
359 *UAS-med27 RNAi* (BL 34576), *UAS-N*^{ACT} (a gift from Helena Richardson), *UAS-ND75*
360 *TRiP* (BL 33911), *UAS-notch RNAi* (VDRC 100002), *UAS-p35* (BL 5072), *UAS-pros RNAi*
361 (BL 26745), *UAS-tll* (a gift from Claude Desplan), *UAS-tll RNAi* (VDRC 330031), *UAS-D*
362 (BL 8861).

363 **Immunostaining**

364 Larval and pupal brains were dissected out in phosphate buffered saline (PBS), fixed in
365 4% formaldehyde for 20 min and rinsed three time in 0.5% PBST (PBS + 0.5% Triton) at
366 room temperature. For immunostaining, brains were incubated in primary antibodies
367 overnight at 4°C, followed by two washes in 0.5% PBST and then an overnight secondary
368 antibody incubation at 4°C or 3 hrs at room temperature. Brains were afterwards rinsed

369 two times in 0.5% PBST and incubated in 50% glycerol in PBS for 20 min. Samples were
370 mounted in 80% glycerol in PBS, on glass slides and sealed with coverslips (22x22 mm,
371 No.1.5, Knittel) for image acquisition. The primary antibodies used were: rat anti-Dpn
372 (1:200, Abcam 195172), chick anti-GFP (1:1000, Abcam 13970), mouse anti-EcR^{common}
373 (1:50, DSHB Ag10.2), rabbit anti-Dcp-1 (1:100, Cell Signalling 95785), rat anti-Mira
374 (1:100, Abcam 197788), rat anti-Pros (a gift from Fumio Matsuzaki), rabbit anti-β-
375 Galactosidase (1:200, a gift from Helena Richardson), rabbit anti-Ase (a gift from Lily Jan
376 and Yuh Nung Jan), mouse anti-Repo (1:50, DSHB 8D12), and rat anti-DE-Cad (1:200,
377 DSHB DCAD2), rabbit anti-PatJ (1:500, a gift from Helena Richardson). Secondary
378 donkey antibodies conjugated to Alexa 555 and Alexa 647, and goat antibodies conjugated
379 to Alexa 405, 488, 555, and 647 (Molecular Probes) were used at 1:500.
380
381 **Imaging and image processing**
382 Images were acquired using Olympus FV3000 confocal microscope with 40x (NA 0.95,
383 UPLSAPO) and 60x (NA 1.30, UPLSAPO) objectives. Δz = 1.5 μm. Images were processed
384 using Fiji (https://imagej.net/Fiji). Single section or maximum projections were shown as
385 representative images in the figures.
386 Quantification was performed in Fiji or via 3D reconstruction in Imaris (Bitplane).
387 For quantifications of NB numbers (Figures 1C, Supplementary Figure 1E, 2E), number of
388 Dpn^+ NBs in the medulla/OL were measured. For quantifications of nuclear sizes of
389 medulla NBs (Figure 1E), nuclear diameters identified by Dpn were measured. For
390 quantifications of the ratio of NBs in clones (Figures 2H, 2K, 3D, 4E, 5L, Supplementary
391 figure 1J, 3H), GFP^+ clones were first detected, and clonal volumes were measured. The
392 GFP^+ areas were then utilised to make a mask for GFP^+Dpn^+ or GFP^+Mira^+ NBs within the
393 clones, which was in turn used to measure the total Dpn volume. The NB ratio in clones
394 is calculated as the ratio of Dpn^+GFP^+ or GFP^+Mira^+ volume over GFP^+ volume. For
395 quantification of the numbers of glia in the medulla (Supplementary Figure 3G), the total
396 numbers of $Repo^+$ cells in the deep section of the medulla were measured in each lobe.
397 For quantification of the NE volumes (Figure 2B), DE-Cad^+ volumes were measured in

each lobe. Images were assembled in Adobe InDesign 2024 and Affinity Publisher 2. Scale bars = 10 μm or 50 μm per indicated in figures.

Statistical analyses

At least two animals per genotype were used for all experiments. Statistical analyses were performed in GraphPad Prism 9. In graphs, data (crossbars) = mean ± standard error of the mean (SEM). n = lobes unless specified. Graphs were plotted using RStudio. For comparisons between two conditions, P-values were calculated by non-parametric Mann-Whitney tests when data show non-normally distribution. For comparisons between more than two conditions, P-values were calculated by either ordinary one-way ANOVA tests for normally distributed data, or Kruskal-Wallis tests for non-normally distributed data. Dunnet or Dunn's tests were used to correct for multiple comparisons following one-way ANOVA and Kruskal-Wallis tests, respectively. *(*) $p<0.05$ (**) $p< 0.01$, (***) $p< 0.001$, (****) $p < 0.0001$, (ns) $p>0.05$*

Acknowledgements

We are grateful to Lei Zhang, Alex Gould, Claude Desplan, Fumio Matsuzaki, Helena Richardson, Yuh Nung Jan for generous sharing of fly stocks and antibodies. We would also like to thank Holger Apitz, Édel Alvarez-Ochoa, and Qian Dong for fruitful discussions and critical reading of the manuscript. We also thank Bloomington Drosophila Stock Centre, Vienna Drosophila Resource Centre, and Developmental Studies Hybridoma Bank for fly stocks and antibodies. We would like to also thank OZDros for *Drosophila* quarantine, Peter MacCallum Cancer Institute CAHM for microscopy assistance. LYC's laboratory is supported by funding from the NHMRC Ideas Grant (APP2011289), and the Peter MacCallum Cancer Foundation.

Disclosure and competing interests statement

The authors declare no competing interests.

References

Ameele J van den & Brand AH (2019) Neural stem cell temporal patterning and brain tumour growth rely on oxidative phosphorylation. *eLife* 8

van den Ameele J & Brand AH (2019) Neural stem cell temporal patterning and brain tumour growth rely on oxidative phosphorylation. *eLife* 8: e47887

Apitz H & Salecker I (2014) A challenge of numbers and diversity: neurogenesis in the Drosophila optic lobe. *J Neurogenet* 28: 233–249

Arain U, Islam IM, Valentino P & Erclik T (2022) Concurrent temporal patterning of neural stem cells in the fly visual system. 2022.10.13.512100 doi:10.1101/2022.10.13.512100 [PREPRINT]

Bello BC, Hirth F & Gould AP (2003) A Pulse of the Drosophila Hox Protein Abdominal-A Schedules the End of Neural Proliferation via Neuroblast Apoptosis. *Neuron* 37: 209–219

Bello BC, Izergina N, Caussinus E & Reichert H (2008) Amplification of neural stem cell proliferation by intermediate progenitor cells in Drosophila brain development. *Neural Development* 3: 5

Boone JQ & Doe CQ (2008) Identification of Drosophila type II neuroblast lineages containing transit amplifying ganglion mother cells. *Dev Neurobiol* 68: 1185–1195

Bowman SK, Rolland V, Betschinger J, Kinsey KA, Emery G & Knoblich JA (2008) The tumor suppressors Brat and Numb regulate transit-amplifying neuroblast lineages in Drosophila. *Dev Cell* 14: 535–546

Choksi SP, Southall TD, Bossing T, Edoff K, de Wit E, Fischer BE, van Steensel B, Micklem G & Brand AH (2006a) Prospero acts as a binary switch between self-renewal and differentiation in Drosophila neural stem cells. *Dev Cell* 11: 775–789

Choksi SP, Southall TD, Bossing T, Edoff K, de Wit E, Fischer BE, van Steensel B, Micklem G & Brand AH (2006b) Prospero acts as a binary switch between self-renewal and differentiation in Drosophila neural stem cells. *Dev Cell* 11: 775–789

Dillard C, Narbonne-Reveau K, Foppolo S, Lanet E & Maurange C (2018) Two distinct mechanisms silence chinmo in Drosophila neuroblasts and neuroepithelial cells to limit their self-renewal. *Development* 145

Egger B, Boone JQ, Stevens NR, Brand AH & Doe CQ (2007) Regulation of spindle orientation and neural stem cell fate in the Drosophila optic lobe. *Neural Dev* 2: 1

Egger B, Gold KS & Brand AH (2010) Notch regulates the switch from symmetric to asymmetric neural stem cell division in the Drosophila optic lobe. *Development* 137: 2981–2987

Freeman MR & Doe CQ (2001) Asymmetric Prospero localization is required to generate mixed neuronal/glial lineages in the Drosophila CNS. *Development* 128: 4103–4112

464 Götz M & Huttner WB (2005) The cell biology of neurogenesis. *Nat Rev Mol Cell Biol* 6:
465 777–788

466 Hakes AE & Brand AH (2020) Tailless/TLX reverts intermediate neural progenitors to stem
467 cells driving tumourigenesis via repression of asense/ASCL1. *eLife* 9: e53377

468 Hara Y, Hirai K, Togane Y, Akagawa H, Iwabuchi K & Tsujimura H (2013) Ecdysone-
469 dependent and ecdysone-independent programmed cell death in the developing optic
470 lobe of Drosophila. *Developmental Biology* 374: 127–141

471 Hara Y, Sudo T, Togane Y, Akagawa H & Tsujimura H (2018) Cell death in neural precursor
472 cells and neurons before neurite formation prevents the emergence of abnormal neural
473 structures in the Drosophila optic lobe. *Developmental Biology* 436: 28–41

474 Harding K & White K (2018a) Drosophila as a Model for Developmental Biology: Stem
475 Cell-Fate Decisions in the Developing Nervous System. *J Dev Biol* 6

476 Harding K & White K (2018b) Drosophila as a Model for Developmental Biology: Stem
477 Cell-Fate Decisions in the Developing Nervous System. *J Dev Biol* 6

478 Homem CCF, Steinmann V, Burkard TR, Jais A, Esterbauer H & Knoblich JA (2014)
479 Ecdysone and mediator change energy metabolism to terminate proliferation in
480 Drosophila neural stem cells. *Cell* 158: 874–888

481 Ito K & Hotta Y (1992a) Proliferation pattern of postembryonic neuroblasts in the brain of
482 Drosophila melanogaster. *Developmental Biology* 149: 134–148

483 Ito K & Hotta Y (1992b) Proliferation pattern of postembryonic neuroblasts in the brain of
484 Drosophila melanogaster. *Developmental Biology* 149: 134–148

485 Konstantinides N, Holguera I, Rossi AM, Escobar A, Dudragne L, Chen Y-C, Tran TN,
486 Martínez Jaimes AM, Özel MN, Simon F, *et al* (2022) A complete temporal
487 transcription factor series in the fly visual system. *Nature* 604: 316–322

488 Lanet E, Gould AP & Maurange C (2013a) Protection of neuronal diversity at the expense of
489 neuronal numbers during nutrient restriction in the Drosophila visual system. *Cell Rep*
490 3: 587–594

491 Lanet E, Gould AP & Maurange C (2013b) Protection of neuronal diversity at the expense of
492 neuronal numbers during nutrient restriction in the Drosophila visual system. *Cell Rep*
493 3: 587–594

494 Leevers SJ, Weinkove D, MacDougall LK, Hafen E & Waterfield MD (1996) The
495 Drosophila phosphoinositide 3-kinase Dp110 promotes cell growth. *EMBO J* 15:
496 6584–6594

497 Li X, Erclik T, Bertet C, Chen Z, Voutev R, Venkatesh S, Morante J, Celik A & Desplan C
498 (2013a) Temporal patterning of Drosophila medulla neuroblasts controls neural fates.
499 *Nature* 498: 456–462

500 Li X, Erclik T, Bertet C, Chen Z, Voutev R, Venkatesh S, Morante J, Celik A & Desplan C
501 (2013b) Temporal patterning of Drosophila medulla neuroblasts controls neural fates.
502 *Nature* 498: 456–462

503 Maurange C, Cheng L & Gould AP (2008) Temporal transcription factors and their targets
504 schedule the end of neural proliferation in Drosophila. *Cell* 133: 891–902

505 Morin X, Daneman R, Zavortink M & Chia W (2001) A protein trap strategy to detect GFP-
506 tagged proteins expressed from their endogenous loci in Drosophila. *Proceedings of*
507 *the National Academy of Sciences* 98: 15050–15055

508 Pahl MC, Doyle SE & Siegrist SE (2019) E93 integrates neuroblast intrinsic state with
509 developmental time to terminate neurogenesis via autophagy. *Current biology : CB*
510 29: 750

511 Ragone G, Bernardoni R & Giangrande A (2001) A Novel Mode of Asymmetric Division
512 Identifies the Fly Neuroglioblast 6-4T. *Developmental Biology* 235: 74–85

513 Riddiford LM (1993) Hormones and Drosophila development. In *The development of*
514 *Drosophila melanogaster* pp 899–939.

515 Rust K, Tiwari MD, Mishra VK, Grawe F & Wodarz A (2018) Myc and the Tip60 chromatin
516 remodeling complex control neuroblast maintenance and polarity in Drosophila.
517 *EMBO J* 37: e98659

518 Sato M, Yasugi T & Trush O (2019) Temporal patterning of neurogenesis and neural wiring
519 in the fly visual system. *Neuroscience Research* 138: 49–58

520 Shaw RE, Kottler B, Ludlow ZN, Buhl E, Kim D, Morais da Silva S, Miedzik A, Coum A,
521 Hodge JJ, Hirth F, *et al* (2018) In vivo expansion of functionally integrated
522 GABAergic interneurons by targeted increase in neural progenitors. *EMBO J* 37:
523 e98163

524 Siegrist SE, Haque NS, Chen C-H, Hay BA & Hariharan IK (2010) Inactivation of both foxo
525 and reaper promotes long-term adult neurogenesis in Drosophila. *Current biology :*
526 *CB* 20: 643

527 Syed MH, Mark B & Doe CQ (2017a) Steroid hormone induction of temporal gene
528 expression in Drosophila brain neuroblasts generates neuronal and glial diversity.
529 *eLife* 6: e26287

530 Syed MH, Mark B & Doe CQ (2017b) Steroid hormone induction of temporal gene
531 expression in Drosophila brain neuroblasts generates neuronal and glial diversity.
532 *eLife* 6: e26287

533 Veen K, Nguyen P-K, Froldi F, Dong Q, Alvarez-Ochoa E, Harvey KF, McMullen JP,
534 Marshall O, Jusuf PR & Cheng LY (2023) Dedifferentiation-derived neural stem cells
535 exhibit perturbed temporal progression. *EMBO reports* 24: e55837

536 Vincent S, Vonesch JL & Giangrande A (1996) Glide directs glial fate commitment and cell
537 fate switch between neurones and glia. *Development* 122: 131–139

538 Wang W, Liu W, Wang Y, Zhou L, Tang X & Luo H (2011) Notch signaling regulates
539 neuroepithelial stem cell maintenance and neuroblast formation in Drosophila optic
540 lobe development. *Developmental Biology* 350: 414–428

541 Xu T, Nicolson S, Denton D & Kumar S (2015) Distinct requirements of Autophagy-related
542 genes in programmed cell death. *Cell Death Differ* 22: 1792–1802

543 Yang C-P, Samuels TJ, Huang Y, Yang L, Ish-Horowicz D, Davis I & Lee T (2017) Imp and
544 Syp RNA-binding proteins govern decommissioning of Drosophila neural stem cells.
545 *Development* 144: 3454–3464

546 Yasugi T, Sugie A, Umetsu D & Tabata T (2010) Coordinated sequential action of EGFR and
547 Notch signaling pathways regulates proneural wave progression in the Drosophila
548 optic lobe. *Development* 137: 3193–3203

549 Yasugi T, Umetsu D, Murakami S, Sato M & Tabata T (2008a) Drosophila optic lobe
550 neuroblasts triggered by a wave of proneural gene expression that is negatively
551 regulated by JAK/STAT. *Development* 135: 1471–1480

552 Yasugi T, Umetsu D, Murakami S, Sato M & Tabata T (2008b) Drosophila optic lobe
553 neuroblasts triggered by a wave of proneural gene expression that is negatively
554 regulated by JAK/STAT. *Development* 135: 1471–1480

555 Zhou Y, Yang Y, Huang Y, Wang H, Wang S & Luo H (2019) Broad Promotes
556 Neuroepithelial Stem Cell Differentiation in the Drosophila Optic Lobe. *Genetics*
557 213: 941–951

558 Zhu H, Zhao SD, Ray A, Zhang Y & Li X (2022) A comprehensive temporal patterning gene
559 network in Drosophila medulla neuroblasts revealed by single-cell RNA sequencing.
560 *Nat Commun* 13: 1247

561

562

563

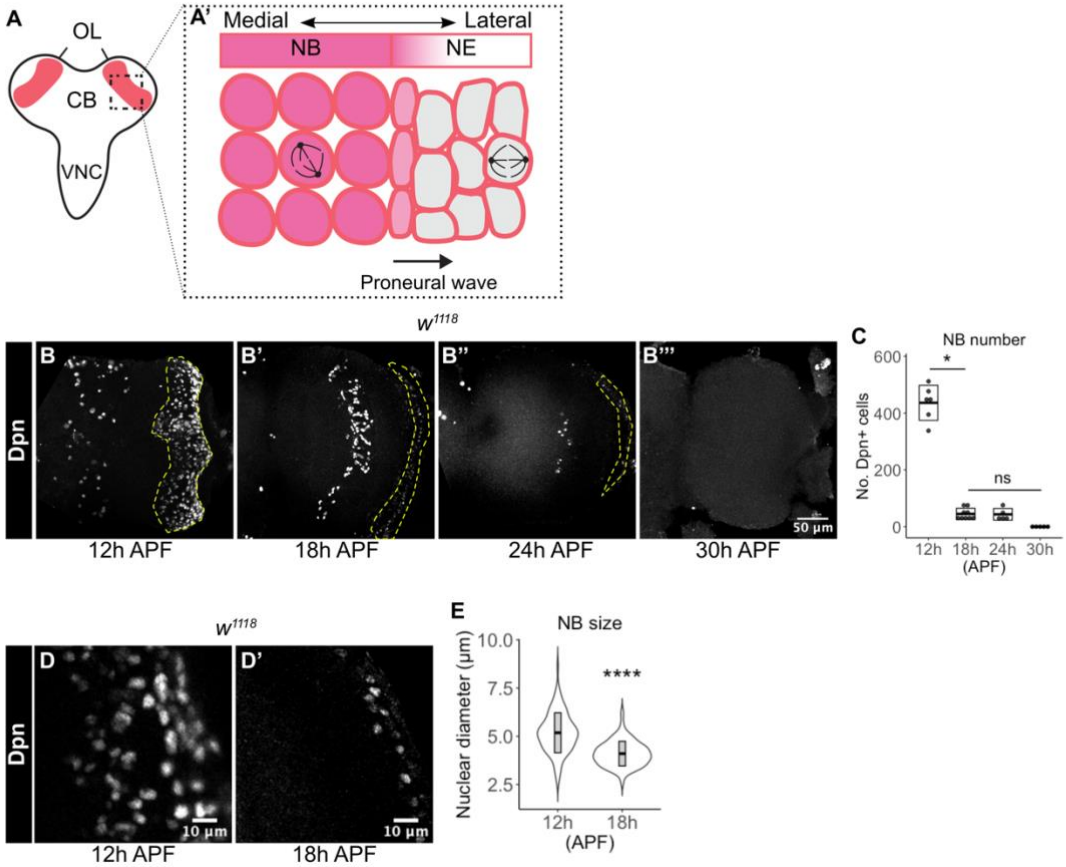

Figure 1: Medulla NBs are terminated during early pupal development.

(A-A') Schematic depicting the larval CNS that is consisted of three main regions: the central brain (CB), the ventral nerve cord (VNC) and the optic lobe (OL). Box area indicates inset shown in A'. (A') The apical view of the outer proliferation centre (OPC) of the OL. Here, NE cells first symmetrically divide to self-renew. At mid-larval development, a proneural wave is initiated and travels from the medial to lateral of the NE. Upon the proneural wave, NE cells differentiate into NBs and switch to asymmetric cell division for neurogenesis.

(B-B''') In the wildtype (w^{1118}) OL, the number of medulla NBs marked by Dpn (dashed lines), gradually reduces from 12 hr to 24 hr APF. Medulla NBs completely disappear at 30 hr APF.

(C) Quantification of the numbers of medulla NBs at 12 hr, 18 hr, 24 hr, 30 hr APF in the wildtype OLs. Kruskal-Wallis test and Dunn's test to correct for multiple comparisons: *p = 0.0314. 12 hr: n = 6, m = 436.3 ± 25.21. 18 hr: n = 9, m = 45.22 ± 6.616. 24 hr: n = 5, m = 43.6 ± 9.255. 30 hr: n = 5, m = 0.000 ± 0.000.

(D-D') In the wildtype, the nuclear size of medulla NBs marked by Dpn decreases from 12 hr to 18 hr APF.

(E) Quantification of the nuclear diameters of medulla NBs at 12 hr and 18 hr APF. Mann-Whitney test: ****p < 0.0001. 12 hr: n = 109 cells, m = 5.182 ± 0.099 µm. 18 hr APF: n = 61 cells, m = 4.100 ± 0.082 µm.

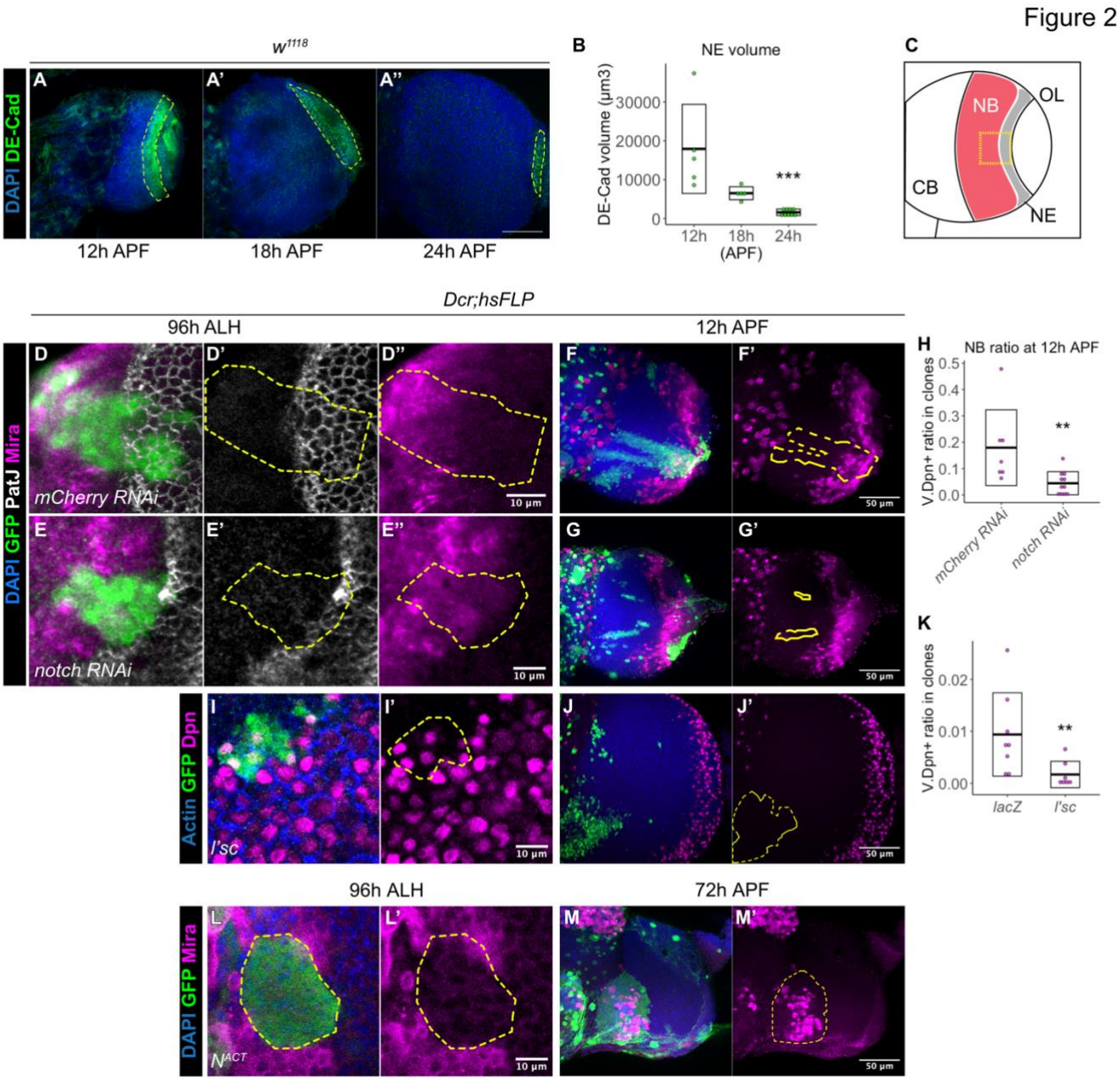

Figure 2: The termination of medulla NBs is scheduled by the timing of the larval NE-NB transition.

(A-A'') The NE pool marked by DE-Cad (green, dashed lines) becomes gradually depleted from 12 hr to 24 hr APF. DAPI (blue)

(B) Quantification of DE-Cad volumes at 12 hr, 18 hr, and 24 hr APF. Kruskal-Wallis test and Dunn's test to correct for multiple comparisons: ***p = 0.0003. 12 hr: n = 5, m = 17922 ± 5129. 18 hr: n = 5, m = 6508 ± 747.0. 24 hr: n = 9, m = 1597 ± 280.9.

(C) Schematic depicting the larval OL at 120 hr ALH, where the NE-NB transition is boxed, and is the region of interest in (D-M).

(D-E') Representative images of *hsFLP* clones (dashed lines) at 120 hr ALH, induced with (D-D'') *UAS-mCherry RNAi* and (E-E'') *UAS-notch RNAi*. GFP (green), PatJ (grey), Mira (magenta).

(F-G') Representative maximum projections of the OL at 12 hr APF, in which *hsFLP* clones (dashed lines) are induced with (F-F') *UAS-mCherry RNAi* and (G-G') *UAS-notch RNAi*. DAPI (blue), GFP (green), Mira (magenta).

(H) Quantification of the NB ratio in clones in the OL at 12 hr APF in which *hsFLP* clones are induced with *UAS-mCherry RNAi* and *UAS-notch RNAi*. Mann-Whitney test: **p = 0.0041. *mCherry RNAi*: n = 7, m = 0.179 ± 0.054. *notch RNAi*: n = 11, m = 0.044 ± 0.013.

(I-I') Representative *hsFLP* clone (dashed line) at 120 hr ALH, induced with *UAS-l'sc*.

(J-J') Representative maximum projections of the OL at 12 hr APF, in which *hsFLP* clones (dashed line) are induced with *UAS-l'sc*. Actin (blue), GFP (green), Dpn (magenta)

(K) Quantification of the NB ratio in clones in the OL at 12 hr APF in which *hsFLP* clones are induced with *UAS-lacZ* and *UAS-l'sc*. Mann-Whitney test: **p = 0.0057. *lacZ*: n = 8, m = 0.009 ± 0.003. *l'sc*: n = 7, m = 0.002 ± 0.001.

(L-L') Representative *hsFLP* clone (dashed line) at 120 hr ALH, induced with *UAS-N^{ACT}*.

(M-M') Representative maximum projections of the OL at 72 hr APF, in which *hsFLP* clones (dashed lines) are induced *UAS-N^{ACT}*. Note that N^{ACT} clones do not generate NBs until late pupal development.

DAPI (blue), GFP (green), Mira (magenta)

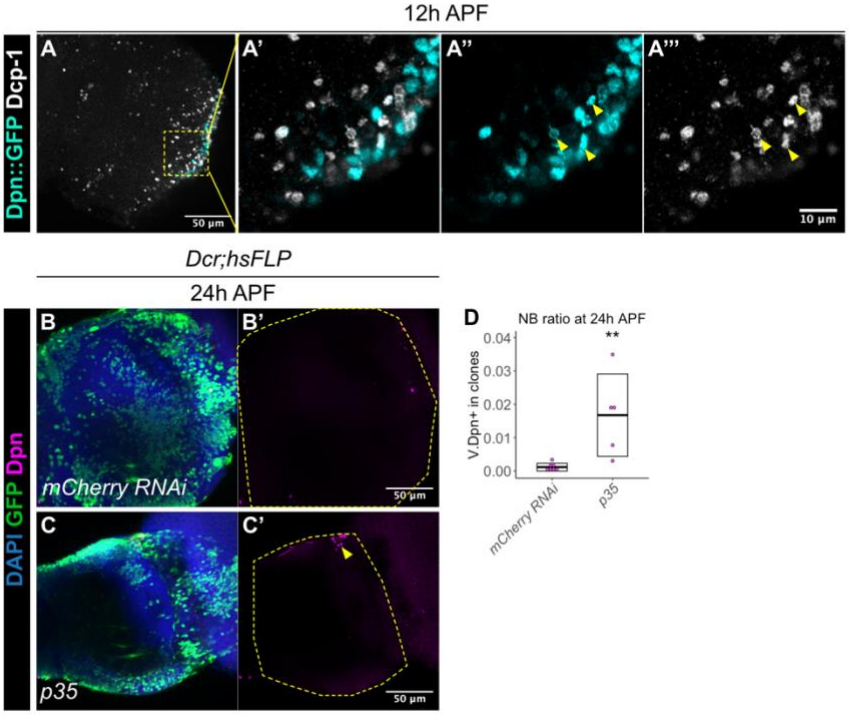

Figure 3: A subset of medulla NBs terminate via cell death.

(A) At 12 hr APF, a subset of medulla NBs marked by Dpn::GFP (cyan) express the apoptotic marker Dcp-1 (grey) (arrowheads). A'-A''' is the magnified view of the boxed inset in A.

(B-C') Representative maximum projections of the OL (dashed line) at 24 hr APF with *hsFLP* clones induced with (B-B') *UAS-mCherry RNAi* and (C-C') *UAS-p35*. Ectopic NBs are indicated by arrowhead. DAPI (blue), GFP (green), Dpn (magenta). The same *hsFLP>mCherry RNAi* representative image is used in Supplementary figure 1F and Figure 4E.

(D) Quantification of the NB ratio in *hsFLP* induced with *UAS-mCherry RNAi* and *UAS-p35* at 24 hr APF in the OL. Mann-Whitney test: **p = 0.005. *mCherry RNAi*: n = 7, m = 0.001 ± 0.0004. *p35*: n = 5, m = 0.017 ± 0.006.

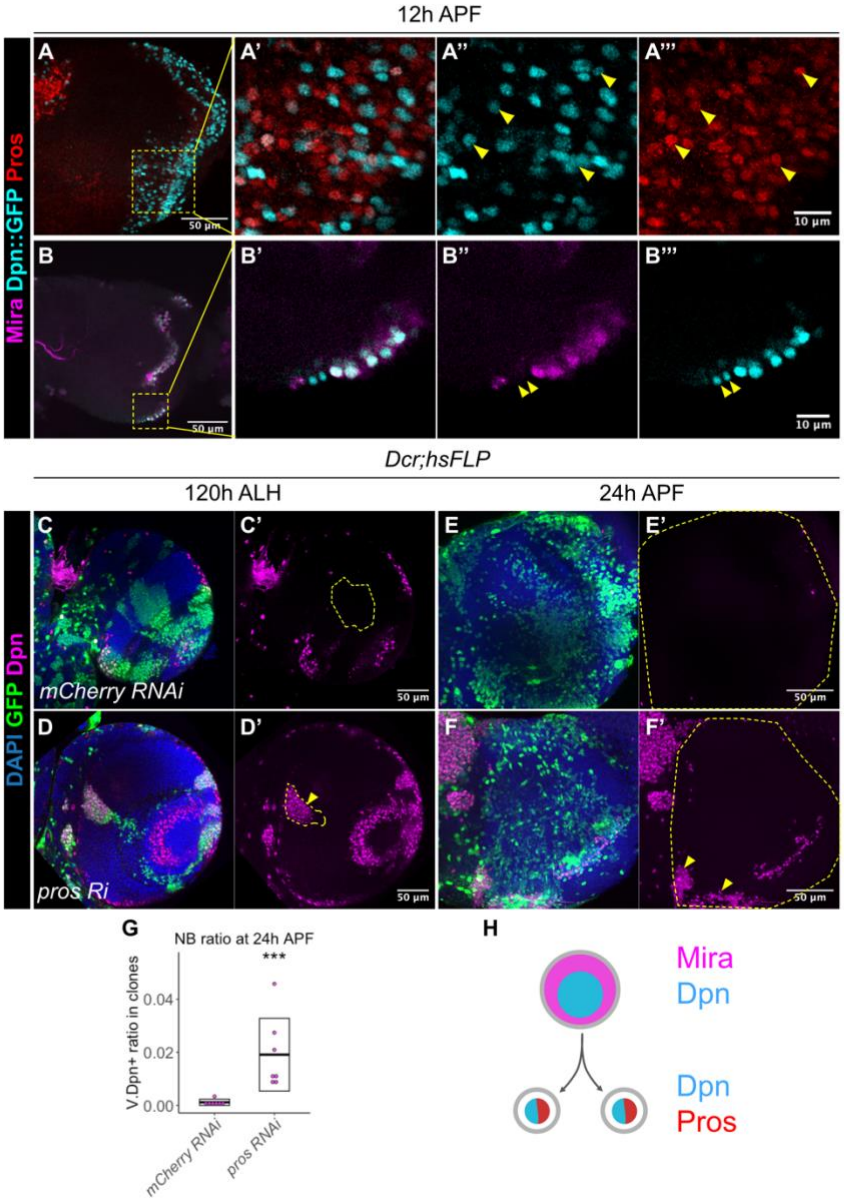

Figure 4: The termination of medulla NBs requires Pros-mediated size symmetric division.

(A-A''') Representative images of the OL at 12 hr APF. Some NBs marked by Dpn::GFP (cyan) in the medulla co-express Pros (red) (arrowheads). A'-A''' are magnified images of boxed inset in A.

(B-B''') Representative images of the OL at 12 hr APF. On the superficial layer where medulla NBs reside, we have occasionally observed a pair of similarly-sized cells at the most medial position (arrowheads), that express Dpn::GFP (cyan) but not Mira (magenta). B'-B''' are magnified images of boxed inset in B.

(C-D') Representative images of the deep layers of the medulla with *hsFLP* clones (dashed lines) driving (C-C) *UAS-mCherry RNAi* and (D-D') *UAS-pros RNAi* at 120 hr ALH. Arrowhead indicates ectopic NBs in the deep section of the medulla.

(E-F') Representative maximum projects of an OL (dashed line) with *hsFLP* clones driving (E-E') *UAS-mCherry RNAi* and (F-F') *UAS-pros RNAi* at 24 hr ALH. Arrowhead indicates

persistent NBs. The same *hsFLP>mCherry RNAi* representative image is used in Supplementary figure 1F and Figure 3B. DAPI (blue), GFP (green), Dpn (magenta).

(G) Quantification of the NB ratio in clones in the OL at 24 hr APF, in which *hsFLP* clones are induced with *UAS-mCherry RNAi* and *UAS-pros RNAi*. Mann-Whitney test: ***p = 0.0006. *mCherry RNAi*: n = 7, m = 0.001 ± 0.0004. *pros RNAi*: n = 7, m = 0.019 ± 0.005.

(H) Schematic depicting a medulla NB expresses nuclear Pros to promote symmetric division.

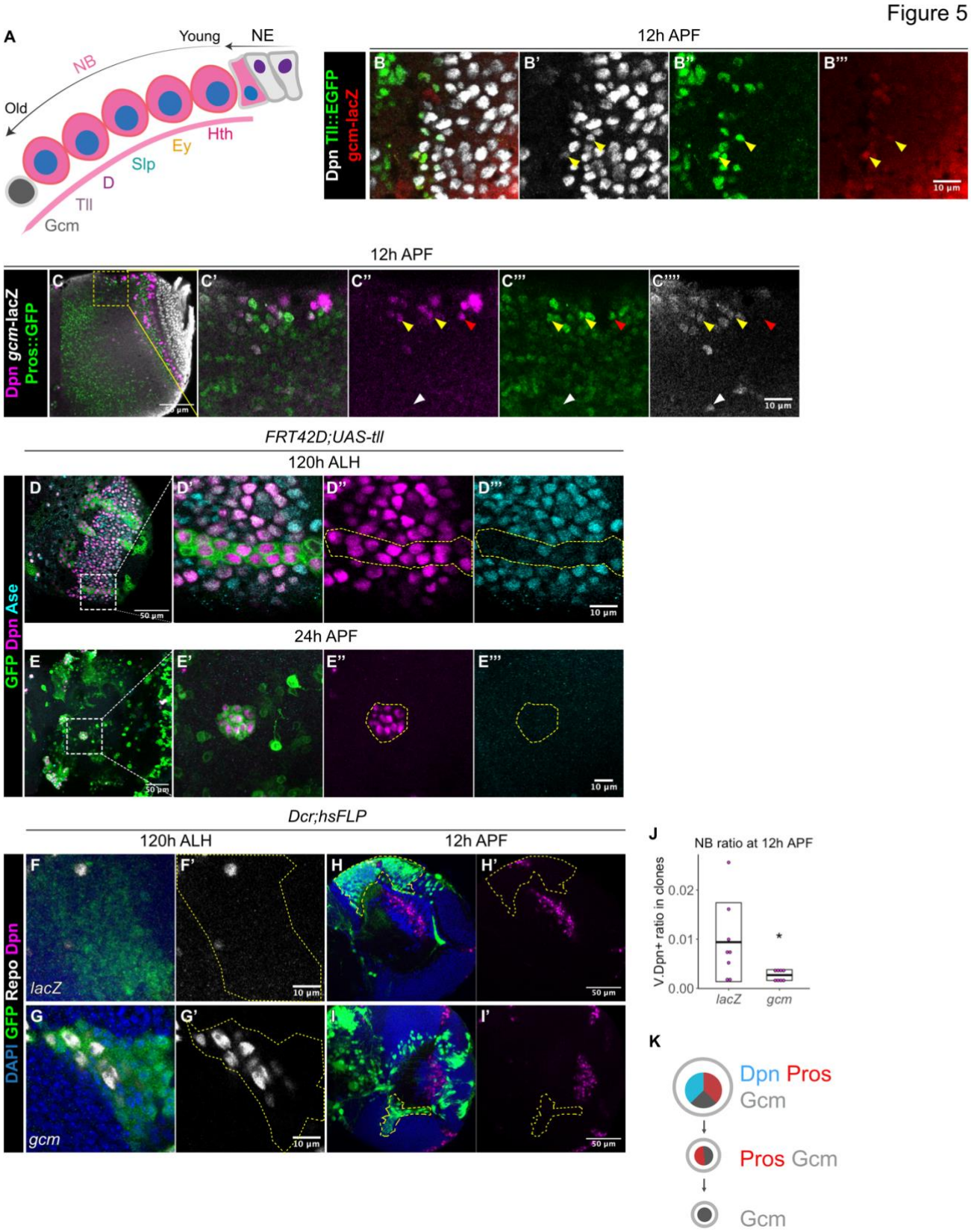

Figure 5: Gcm is sufficient to induce gliogenesis in the medulla at the expense of NBs.

(A) Schematic of the temporal progression in the OL medulla.

(B-B'''') Representative images of the superficial layer of the medulla NBs at 12 hr APF. Some of the most medial NBs (arrowheads) express Dpn (gray), Tll::EGFP (green), and *gcm*-lacZ (red).

(C-C’’’’) Representative images of the OL at 12 hr APF. Here, some of the most medial NBs are $Dpn^{+}Pros^{+}gcm^{+}$ (yellow arrowheads) whereas some are $Dpn^{+}Pros^{+}gcm^{-}$ (red arrowheads) on the superficial layers. In the deep layers, some cells are $Dpn^{-}Pros^{-}gcm^{+}$ (white arrowheads). C’-C’’’ are magnified images of C.

(D-D’’’) Representative images of the OL at 120 hr ALH, in which MARCM clones overexpressed for Tll are induced. Box indicates inset shown in L’-L’’’. In the clone (dashed line), medulla NBs expressed low levels of Ase compared to wildtype medulla NBs outside of the clone. D’-D’’’ are magnified images of D.

(E-E’’’) Representative maximum projections of the OL at 24 hr APF, in which MARCM overexpressed for Tll are induced. In the clone (dashed line), ectopic NBs do not express Ase. E’-E’’’ are magnified images of E. GFP (green), Dpn (magenta), Ase (cyan).

(F-G’) Representative *hsFLP* clones (dashed lines) induced with (F-F’) *UAS-lacZ*, and (G-G’) *UAS-gcm* at 120 hr APF.

(H-I’) Representative images of the OLs (dashed lines) at 12 hr APF, in which *hsFLP* clones are induced with (H-H’) *UAS-lacZ*, and (I-I’) *UAS-gcm*.

(J) Quantification of the NB ratio in clones in the OLs at 12 hr APF, in which *hsFLP* clones are induced with *UAS-lacZ* and *UAS-gcm*. Mann-Whitney test: *$p = 0.0379$. *lacZ*: $n = 8$, $m = 0.009 \pm 0.003$. *gcm*: $n= 8$, $m = 0.003 \pm 0.0004$.

(K) Schematic depicting a Dpn^{+} medulla NB expresses nuclear Pros and the glial cell fate determinant Gcm to induce a switch from neurogenic-to-gliogenic program.

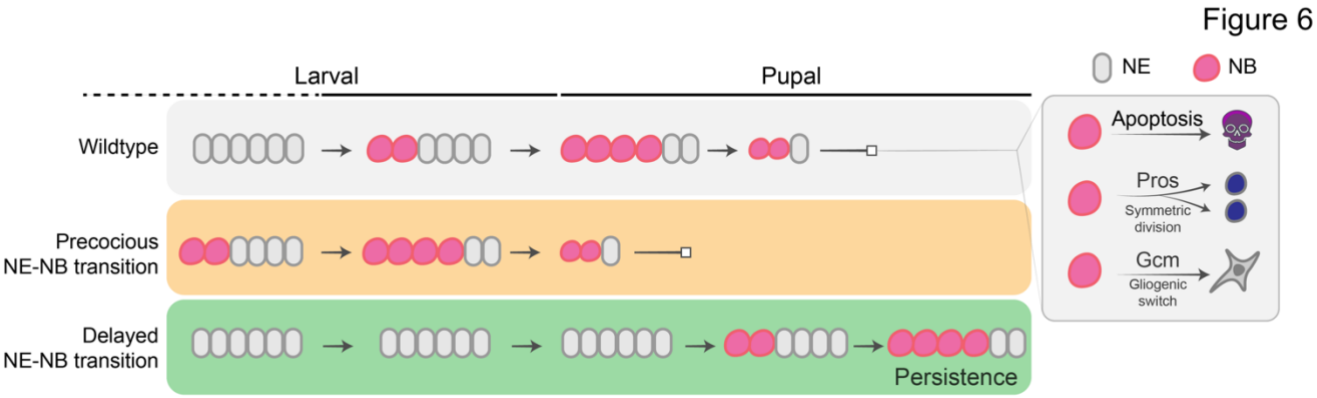

Figure 6: Working model of the termination of medulla NBs.

Timing of NB termination in the early pupal stages is scheduled by the timing of the NE-NB transition in the larval stages. Medulla NBs can be terminated via three mechanisms: (1) cell death, (2) Pros-mediated symmetric division and (3) Gcm-mediated gliogenic switch of the NBs.